

HADRON COLLIDER POTENTIAL FOR EXCITED BOSONS SEARCH

M. V. Chizhov^{1,2}, *I. R. Boyko*¹,
*V. A. Bednyakov*¹, *J. A. Budagov*¹

¹ Joint Institute for Nuclear Research, Dubna

² Centre for Space Research and Technologies, Faculty of Physics, Sofia University, Sofia

INTRODUCTION	904
SIGNAL AND BACKGROUND SAMPLES	907
EXCLUSION LIMIT SETTING AND DISCOVERY POTENTIAL ESTIMATION	911
Exclusion Limits	911
Discovery Potential	912
Systematic Errors	913
EXCLUSION LIMITS AT $\sqrt{s} = 7$ TeV AND COMPARISON WITH OFFICIAL ATLAS RESULTS	913
EXCLUSION LIMITS AT $\sqrt{s} = 8$ TeV	916
THE DISCOVERY POTENTIAL AND THE EXCLUSION LIMITS AT $\sqrt{s} = 13$ TeV AND $\sqrt{s} = 14$ TeV	918
THE DISCOVERY POTENTIAL AND THE EXCLUSION LIMITS AT $\sqrt{s} = 33$ TeV	920
CONCLUSION	921
REFERENCES	921

HADRON COLLIDER POTENTIAL FOR EXCITED BOSONS SEARCH

M. V. Chizhov^{1,2}, *I. R. Boyko*¹,

*V. A. Bednyakov*¹, *J. A. Budagov*¹

¹ Joint Institute for Nuclear Research, Dubna

² Centre for Space Research and Technologies, Faculty of Physics, Sofia University, Sofia

The e^+e^- and $\mu^+\mu^-$ dilepton final states are the most clear channels for a new heavy neutral resonance search. Their advantage is that usually in the region of expected heavy-mass resonance peak the main irreducible background, from the Standard Model Drell–Yan process, contributes two orders of magnitude smaller than the signal.

In this paper, we consider the future prospects for search for the excited neutral Z^* bosons. The bosons can be observed as a Breit–Wigner resonance peak in the dilepton invariant mass distributions in the same way as the well-known extra gauge Z' bosons. However, the Z^* bosons have unique signatures in transverse momentum, angular and pseudorapidity distributions of the final leptons, which allow one to distinguish them from the other heavy neutral resonances.

At present, only the ATLAS Collaboration has looked for such new excitations at the Large Hadron Collider and has published its results for 7 TeV collision energy. After successful comparison of our evaluation with these official results, we present our estimations for the discovery potential and the exclusion limits on the Z^* -boson search in pp collisions at higher centre-of-mass energies and different luminosities. In particular, LHC Run 2 can discover Z^* boson with its mass up to 5.3 TeV, while the High Luminosity LHC can extend that reach to 6.2 TeV. The High Energy LHC (with collision energy of 33 TeV) will be able to probe two times heavier resonance masses at the same integrated luminosities.

Дилептонные конечные состояния e^+e^- и $\mu^+\mu^-$ являются наиболее чистыми каналами для поиска тяжелых нейтральных резонансов. Их преимущество заключается в том, что основной неустраняемый фон от процесса Дрелла–Яна в районе предполагаемого резонансного пика обычно дает вклад на два порядка меньше величины сигнала.

В этой работе рассматриваются возможности поиска возбужденных нейтральных Z^* -бозонов. Такие бозоны могут быть обнаружены как резонансные пики в распределениях дилептонной инвариантной массы подобно хорошо известным дополнительным калибровочным бозонам Z' . При этом Z^* -бозоны имеют уникальную сигнатуру в распределениях поперечных импульсов, углов и псевдобыстрот конечных лептонов, что позволяет отличить их от других тяжелых нейтральных резонансов.

К настоящему времени только коллаборация ATLAS проводила поиск таких новых возбужденных состояний на Большом адронном коллайдере и опубликовала результаты для энергии столкновений 7 ТэВ. В работе дается оценка экспериментальной чувствительности таких поисков в pp -столкновениях при 7 ТэВ, хорошо согласующаяся с опубликованными результатами. Далее приводятся аналогичные оценки для более высоких энергий при различных светимостях. В частности, во втором сеансе работы Большого адронного коллайдера возможно обнаружение

Z^* -бозона с массой до 5,3 ТэВ (или до 6,2 ТэВ в варианте сверхвысокой светимости). При сверхвысокой энергии столкновений (33 ТэВ) возможно обнаружение вдвое более тяжелых бозонов при той же интегральной светимости.

PACS: 14.70.Pw; 29.20.db

INTRODUCTION

The idea of compositeness of the nature is not new. However, in order to explore the internal structure of the matter, the high-energy colliders are necessary. That is why, for example, search for hypothetical *excited fermions* ψ^* has been fulfilled at all powerful colliders, such as LEP [1], HERA [2], Tevatron [3] and continues at the LHC [4, 5].

The excited fermions have anomalous (magnetic moment type) couplings with the known fermions ψ and the gauge bosons (such as gluons, photons and weak W and Z bosons):

$$\mathcal{L}_{\text{excited}}^{\psi^*} = \frac{g}{2\Lambda} \bar{\psi}^* \sigma^{\mu\nu} \psi (\partial_\mu Z_\nu - \partial_\nu Z_\mu) + \text{h.c.} \quad (1)$$

The parameter Λ is connected to the compositeness mass scale of the new physics. Due to the anomalous type of couplings, the excited fermions have a unique experimental signature for their detection.

The interaction given in (1) could also be reinterpreted from a different point of view, introducing a new *excited boson* Z^* [6]

$$\mathcal{L}_{\text{excited}}^{Z^*} = \frac{g}{2\Lambda} \bar{\psi} \sigma^{\mu\nu} \psi (\partial_\mu Z_\nu^* - \partial_\nu Z_\mu^*) \quad (2)$$

instead of the fermionic excited state ψ . Such a type of new heavy Z^* bosons could also be interesting objects for experimental searches due to their different couplings to the ordinary fermions in comparison with the minimal gauge couplings of Z' bosons. In this paper, we are focused on the search for the excited bosons Z^* , rather than on the well-known Z' bosons from various benchmark models.

In contrast with the minimal gauge couplings, where either only left-handed or right-handed fermions participate in the interactions, the tensor currents (2) mix both left-handed and right-handed fermions. Therefore, like the Higgs particles, the excited bosons carry a nonzero chiral charge and according to the symmetry of the Standard Model they should be introduced as the electroweak doublets ($Z^* W^*$) [7] with the internal quantum numbers identical to the Standard Model Higgs doublet:

$$\mathcal{L} = \frac{g}{M} (\partial_\mu W_\nu^{*-} - \partial_\nu \bar{Z}_\mu^*) \overline{D}_R \sigma^{\mu\nu} \begin{pmatrix} U_L \\ D_L \end{pmatrix} + \frac{g}{M} (\overline{U}_L D_L) \sigma^{\mu\nu} D_R \begin{pmatrix} \partial_\mu W_\nu^{*+} \\ \partial_\mu Z_\nu^* \end{pmatrix}. \quad (3)$$

Here, g is the coupling constant of the $SU(2)_W$ weak gauge group; the compositeness mass scale Λ is chosen to equal the boson mass M ; and U and D generically denote up-type and down-type leptons and quarks*. The coupling constant is chosen in such a way that in the Born approximation all partial fermionic decay widths of the well-known hypothetical W' boson with the SM-like interactions and the charged $W^{*\pm}$ boson with the same mass are identical.

In (3), we have introduced only interactions with the down-type right-handed singlets, D_R . The corresponding Z^* bosons are called «down-type» excited neutral bosons. In the same way as in many of the SM extensions, several Higgs doublets are introduced, the realistic model could include several gauge doublets containing also «up-type» Z^* bosons. However, such bosons interact only with up-type quarks and neutrinos and, therefore, cannot be observed in clear Drell–Yan channel. We do not consider them in the paper.

The bosons, coupled to the tensor quark currents, are some types of excited states as far as the only orbital angular momentum with $L = 1$ contributes to the total angular moment, while the total spin of the system is zero. This property manifests itself in their derivative couplings to fermions and in the different chiral structure of the interactions in contrast to the minimal gauge interactions.

The existence of such doublets with masses not far from the weak scale is motivated by the hierarchy problem [8]. The effective interaction (2) is induced by quantum loop corrections from a renormalizable underlying theory and represents the lowest order effective Lagrangian for the excited bosons interacting with the Standard Model fermions. The corresponding reference model is described in [9].

Compared to the other heavy bosons, interactions mediated by (Z^*W^*) doublets are additionally suppressed in the low-energy processes by powers of small ratio of the momentum transfer to the parameter Λ . Thus, the search for the excited bosons is especially motivated at the LHC and future colliders and at present is conducted by the ATLAS Collaboration [10, 11]. Besides this, the derivative couplings lead to unique signatures for detection of such bosons at the hadron colliders. Decay products of the excited bosons possess previously unexplored angular distribution, which leads to a new strategy of the resonance search in dilepton [12] and dijet [13] final-state channels.

The crucial variable, which can help one to separate the decay distribution from the other resonances, is an absolute value of the pseudorapidity difference between the two final-state fermions $\Delta\eta \equiv |\eta_1 - \eta_2|$ (see Fig. 1). The decay

*Here we assume also universality of lepton and quark couplings with different flavors.

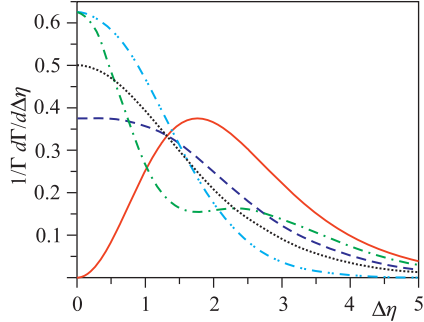


Fig. 1. The normalized angular final-state fermion distributions as functions of $\Delta\eta$ for the scalar (dotted), spin-1 bosons with the minimal couplings (dashed), the excited bosons (solid) and spin-2 resonances, produced through quark (dash-dotted) and gluon (dash-double-dotted) fusion, are shown

distributions of all other resonances have the kinematic absolute maximum at $\Delta\eta = 0$, while the excited-bosons decay distribution is zero at this point and peaks at $\Delta\eta = \ln(3 + \sqrt{8}) \approx 1.76$. The latter corresponds to the polar angle $\theta = 45^\circ$ between direction of the two final fermions in the resonance rest frame and the beam direction. It contradicts a little bit to the common opinion about new physics signal expectations at $\theta = 90^\circ$.

The background from the Standard Model Drell–Yan (DY) process, originated from the intermediate γ and Z boson, which have the minimal gauge couplings with quarks and leptons, contributes mainly to the central pseudorapidity region $\Delta\eta \approx 0$. The background can be suppressed up to 40% with appropriate cut $\Delta\eta > \Delta\eta_{\min} \approx 1.0$ leaving the main part of the Z^* -signal intact. This feature allows one to enhance the significance of the bump search and identification of the excited bosons in the dilepton final-state channels [12].

However, for the dijet final states, the huge QCD background is exponentially dominated at high $\Delta\eta$ due to the t -channel gluon exchanges, which possess the Rutherford-like distribution $1/(1 - \cos\theta)^2$. It is the reason for the ATLAS and CMS Collaborations to apply a severe cut from above $\Delta\eta < \Delta\eta_{\max} \approx 1.2\text{--}1.3$ [5]. Such a low value of $\Delta\eta_{\max}$ is optimal for resonance searches with nearly isotropic decay distributions, but is not optimal for the excited bosons, where the most of the signal is removed by this restriction. Therefore, in order to optimize the signal significance for the excited bosons, the corresponding cut should be elevated [13] even allowing more background events.

Therefore in this paper, we investigate a hadron collider potential for excited bosons search in the most clear (dilepton) final-state channels. Usually, using these channels leads to more severe constraints on resonance mass than one can extract from dijets channels. We compare our evaluations with the official ATLAS Collaboration results at 7 TeV [10], and after very satisfactory agreement we present our expectations for higher center-of-mass energies of the pp collisions and different (higher) luminosities.

1. SIGNAL AND BACKGROUND SAMPLES

In order to generate signal and background samples we use the CalcHEP package [14]. Although the package allows one to perform calculations only in Born (LO) approximation, using the same generator provides some uniformity between signal and background generation. With its batch and web-interface facilities, the CalcHEP has become user-friendly program. Besides this, the High-Energy Physics Model DataBase (HEPMDB) system [15] and IRIDIS High Performance Computing cluster at the University of Southampton provide access to different theoretical models and fast computer nodes. The authors acknowledge the use of these facilities in the completion of this work.

For the excited-boson signal simulations, the simplified reference model of [9] was used. In the model there are two types of neutral Z^* bosons. One of them couples only to up-type quarks, while the other one couples to down-type quarks and charged leptons only. Therefore, we will consider only the «down-type» Z^* boson, because only this boson can be produced at hadron colliders (due to its interaction with the d -type quarks) and can be detected due to its decay into final state with pair of charged leptons. To investigate numerically the dependence of the Z^* -resonance shape in the invariant dilepton mass distribution (as well as some other observables) on mass M of the Z^* boson, many signal samples should be generated. To this end, the template technique of [16] was applied to both signal and background samples. It allows us to generate only one sample both for signal and for background. The necessary signal distributions for fixed Z^* pole mass M can be obtained by reweighting the corresponding samples. This universal signal template sample is generated without the Breit–Wigner Z^* pole mass factor

$$\text{BW}(m) = \frac{1}{(m^2 - M^2)^2 + (\Gamma M)^2}, \quad (4)$$

where Γ is the Z^* -boson width and m is the dilepton invariant mass. The sample distribution monotonically decreases with increasing m due to decreasing of the parton luminosity (Fig. 2, *a*) and it has proper angular distribution of the dilepton pair from the Z^* boson decay (Fig. 2, *b*). The background distribution falls very quickly with increasing m and cannot provide enough events for our analysis in the region of rather large values of m (in particular, for $m = 2\text{--}4$ TeV).

To compensate this falling effect and to perform the analysis reliably in the region of high dilepton invariant masses having only one sample, the additional enhancing function

$$f(m) = m^\alpha \exp(\beta m) \quad (5)$$

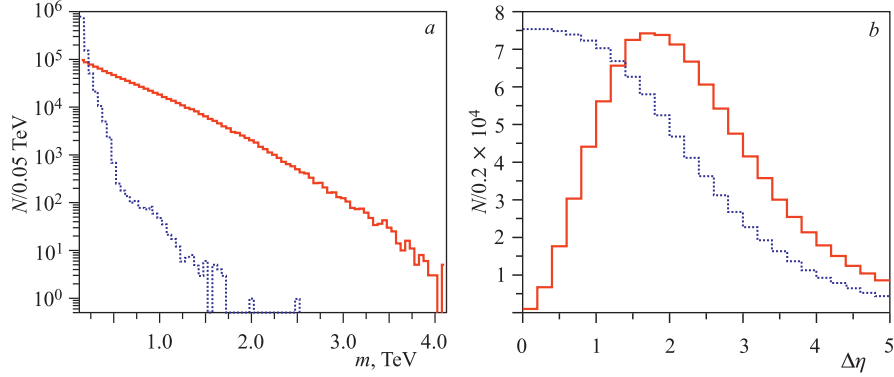


Fig. 2. The invariant mass (a) and the pseudorapidity difference (b) distributions are shown for the signal sample obtained without the Breit–Wigner pole mass factor (solid) and the background sample (dotted) both containing 1M of events generated at $\sqrt{s} = 8 \text{ TeV}$

was used both for signal and background samples. The correction can be realized with CalcHEP user function `usrFF.c`. It is fulfilled to ensure the same relative errors in reweighted samples regardless of the resonance pole mass. This can be achieved by choosing the constants α and β from (5) in such a way that the resulting template distribution decreases inversely with the invariant mass, namely, like C/m . Therefore, the template distribution becomes as flat as possible in logarithmic invariant mass scale (see Fig. 3).

Since the total Z^* resonance decay width into fermions is proportional to the resonance mass M (g is the $SU(2)_W$ gauge coupling)

$$\Gamma = \frac{g^2}{4\pi} M \approx 0.034M, \quad (6)$$

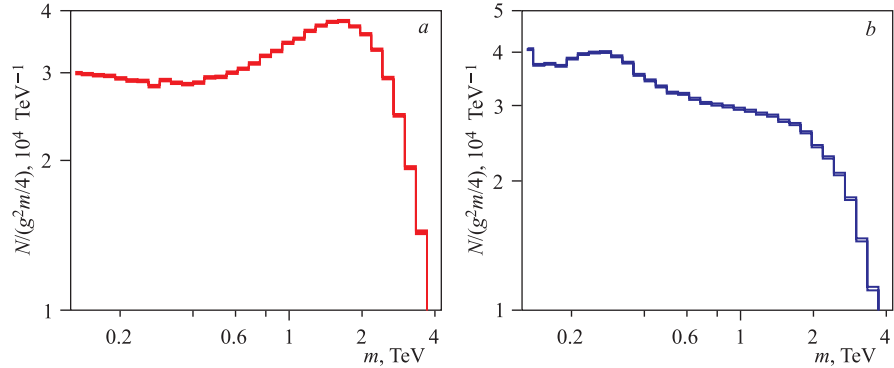


Fig. 3. The corrected signal Z^* (a) and background (b) templates distributions at $\sqrt{s} = 8 \text{ TeV}$

the dimensionless variable $x = m/M$ can be introduced in the Breit–Wigner pole mass factor (4). Then the total number of events and the absolute error after reweighting can be estimated in the resonance vicinity $x \sim 1$ as follows:

$$N_{\text{rew}} \simeq \frac{f^{-1}(M)}{M^4} \int_0^{\infty} \frac{C dx}{(x^2 - 1)^2 + (g^2/4\pi)^2}, \quad (7)$$

$$dN_{\text{rew}} \simeq \frac{f^{-1}(M)}{M^4} \sqrt{\int_0^{\infty} \frac{C dx}{[(x^2 - 1)^2 + (g^2/4\pi)^2]^2}}. \quad (8)$$

It is valid only for narrow resonances and a detector with infinitely good resolution. Here constant $C = N/\ln(M_{\text{max}}/M_{\text{min}})$ is expressed through the total number of generated events N in the template sample. From (7) and (8) one can conclude that the relative error in the reweighted sample will be approximately the same for any resonance mass M from the range $[M_{\text{min}}, M_{\text{max}}]$ and is proportional to

$$\frac{dN_{\text{rew}}}{N_{\text{rew}}} \simeq \frac{2}{g} \sqrt{\frac{\ln(M_{\text{max}}/M_{\text{min}})}{N}}. \quad (9)$$

Since the relative error does not depend on the resonance mass, the reweighted procedure can be applied for any mass with the same accuracy.

In Fig. 3, the obtained nearly logarithmically flat signal and background template distributions at $\sqrt{s} = 8$ TeV are shown, both containing 1M events in the range (0.125 TeV, 4.125 TeV). The special bin size $g^2 m/4 \approx 0.1m$ is selected to show the number of events, which dedicated sample for a fixed pole mass should contain in order to achieve a comparable precision with the reweighted sample from the given template (see Eq. (9)). To validate this statement, a comparison between distributions for dedicated signal sample of 2.5 TeV pole mass resonance containing 30k events and our reweighted signal template sample produced at $\sqrt{s} = 8$ TeV collision energy is shown in Fig. 4.

To derive the exclusion limits and the discovery potential, we should compare our signal with the background. To this end, the simplest «number counting» approach is adopted, which is based on direct comparison of the expected rate of events for the signal and the background processes. From these rates, assuming the Poisson statistics, one can determine the probability that background fluctuations produce a signal-like result according to some estimator, e.g., the likelihood ratio.

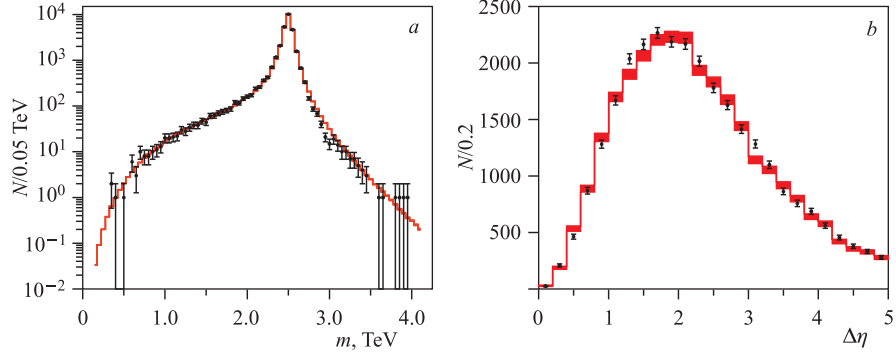


Fig. 4. Comparison is shown between the invariant mass (*a*) and the pseudorapidity difference (*b*) distributions for dedicated sample of 2.5 TeV pole mass resonance (points with error bars) and our reweighted template sample (histograms) at $\sqrt{s} = 8$ TeV

For the narrow resonances, the bulk of events populates the vicinity around the peak $[M - k\Gamma, M + k\Gamma]$. The relative ratio of the signal events in this region to the total number of signal events can be estimated using (4) as

$$s = \frac{\int_{M-k\Gamma}^{M+k\Gamma} BW(m) dm}{\int_0^{\infty} BW(m) dm} \simeq \frac{2 \arctan(k)}{\pi}. \quad (10)$$

If we assume that the background contribution is proportional to the size of the on-peak region $b \sim k$, we can estimate analytically the maximum of the signal significance as a function of k using the formula from Appendix A of [17]:

$$S_{\text{CL}} = \sqrt{2 \left((s+b) \ln \left(1 + \frac{s}{b} \right) - s \right)}, \quad (11)$$

which follows directly from the Poisson distribution of signal events. We will use this equation for estimation of the discovery potential. The corresponding curves as functions of the window size k are shown in Fig. 5. The middle (solid) curve reaches maximum at $k \simeq 3$ for the signal-to-background ratio $s/b \simeq 43.8$, which corresponds, for example, to the Z^* -resonance production with its mass $M = 3.25$ TeV at $\sqrt{s} = 8$ TeV. The upper and lower curves correspond to 10 times higher and smaller the signal-to-background ratios, respectively. They reach maxima at a little bit higher and smaller size windows than the middle curve, respectively. Our results here are in good agreement with the direct numerical calcula-

tions (see Fig. 2 from [18]). As far as the maximum shape is almost flat and has weak sensitivity to k variation, in the following analysis we will use the average optimal value $k = 3$.

Here we have to notice that contrary to the dielectron final states in the muon decay channel, the experimental p_T resolution becomes worse for the high muon momenta (i.e., the error in the muon p_T measurement increases as a function of p_T^2). Therefore, at some (rather high) muon energy we cannot neglect anymore the finite value of the experimental resolution in comparison with the resonance width, which increases linearly with the resonance mass in accordance with (6).

In this case, we cannot choose the optimal window due to the experimental resolution only and have to increase it allowing the presence of more background events. The feature directly affects the discovery potential and the expected exclusion limits derived from the muon and combined channels.

2. EXCLUSION LIMIT SETTING AND DISCOVERY POTENTIAL ESTIMATION

The analysis presented in this paper follows a simplified approach. The observation is reduced to a single value, the total number of events observed in a window around the hypothetical mass of a new resonance. Within this approach, the probability $P(N)$ to observe a given number of events N follows the Poisson distribution:

$$P(N; \mu) = \frac{e^{-\mu} \mu^N}{N!}. \quad (12)$$

Here μ is the average expected value. In the absence of any signal it equals the expected number of background events, $\mu = b$. If a new particle does exist and is expected to produce s signal events in the window, then μ is a sum of the background and the signal, $\mu = s + b$.

In a real experiment, the observed number of events N is compared with both expectations, b and $s + b$, and either an exclusion limit on the possible signal is set or a discovery of a new particle is claimed. In this paper, we evaluate the Z^* -boson experimental potential for both the scenarios.

2.1. Exclusion Limits. The existence of a signal can be excluded when the observed number of events N is inconsistent with the sum of expected signal and

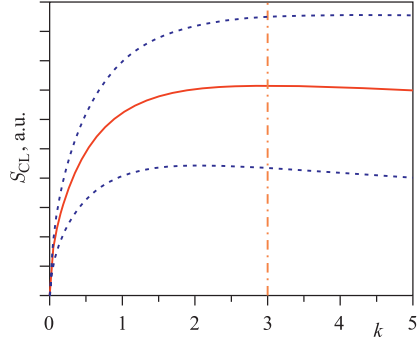


Fig. 5. The signal significance curves for different signal-to-background ratios as a function of the window size k . For example, the middle (solid) curve has $s/b \simeq 43.8$

background. Such (in)consistency can be expressed as the probability to observe the given number of events N or less while $s + b$ events are expected:

$$\text{CL}_{s+b} = P(n \leq N | s + b). \quad (13)$$

However, such definition does not take into account the possibility of strong negative fluctuations when the observed number of events is inconsistent both with the «signal + background» and with «background-only» hypotheses. This problem is handled by the so-called modified frequentist confidence level CL_s :

$$\text{CL}_s = \frac{\text{CL}_{s+b}}{\text{CL}_b}, \quad (14)$$

where $\text{CL}_b = P(n \leq N | b)$ is the probability to observe the given number of events or less in the presence of background only.

The small values of CL_s correspond to the case when the experimental data is more consistent with the background-only hypothesis than with the presence of a signal. The value $1 - \text{CL}_s$ is used to quote the confidence at which the signal hypothesis is excluded. In this paper, we use 95% exclusion limits, i.e., the signal is excluded when $\text{CL}_s < 5\%$.

In the following, we estimate the possible exclusion limits for future experiments. Since the observed number of events is unknown, we estimate the average expected exclusion limit. The background-only hypothesis is assumed and the probability to observe any given number of events $P(N|b)$ is calculated. For given observed number of events N , the signal exclusion limit $X(N)$ is calculated and the average value

$$\langle X \rangle = \sum_{N=0}^{\infty} X(N) P(N|b) \quad (15)$$

is quoted as the average expected exclusion limit. This average exclusion limit rather than a median one is used to avoid an influence of large fluctuations due to the very small number of signal and background events available.

2.2. Discovery Potential. The discovery potential is the possibility of an experiment to rule out the background-only hypothesis by observing a significant excess of events over the background-only expectation. Traditionally the significance is expressed through the number of standard deviations.

In the case of a high-statistics event counting experiment, the Poisson and the Gaussian distributions coincide and the signal significance is expressed simply as

$$S = s/\sqrt{b}. \quad (16)$$

In this paper, we explore the experimental situation with typically very small numbers of both background and signal events. Therefore, we use the significance estimation based on likelihood ratio (11), as proposed in [17].

Traditionally the discovery criteria are more stringent than the signal exclusion ones. Typically signal is excluded at the 95% confidence level (equivalent to 1.6 standard deviations one-sided limit). At the same time, at least five-standard-deviations significance is usually required to claim a discovery. This corresponds to $2.9 \cdot 10^{-7}$ probability of the background fluctuation. We will use the five-standard-deviations criterion to estimate the discovery potential.

2.3. Systematic Errors. The correct estimations of the expected signal and background are affected by the systematic errors. These uncertainties originate from the theory limitations and from the imperfect understanding of the experimental apparatus.

The systematic errors are assumed to have Gaussian distribution, and the probabilities to observe a given number of events are calculated by integrating over the possible values of expected signal and background. In particular, the probability $P(N; s + b)$ to observe N events in (12) is replaced by a new value

$$P'(N; s + b) = \frac{\int_0^\infty ds' \int_0^\infty db' P(N; s' + b') G(s - s', \sigma_s; b - b', \sigma_b)}{\int_0^\infty ds' \int_0^\infty db' G(s - s', \sigma_s; b - b', \sigma_b)}, \quad (17)$$

where $G(s, \sigma_s; b, \sigma_b)$ is a two-dimensional Gaussian distribution centered at point (s, b) with standard deviations σ_s and σ_b , which represent the uncertainties of the estimated signal and background levels.

The presence of the systematic errors reduces the experimental capability both to discover and to exclude a possible signal. In this paper, only for exclusion limits calculations the systematic uncertainties have been taken into account.

3. EXCLUSION LIMITS AT $\sqrt{s} = 7$ TeV AND COMPARISON WITH OFFICIAL ATLAS RESULTS

At present, the ATLAS Collaboration only is looking for the excited Z^* bosons at the LHC [10, 19]. In 2011, the ATLAS Collaboration collected 4.9 and 5.0 fb^{-1} of integrated statistics in dielectron and dimuon final-state channels, respectively, at center-of-mass energy of 7 TeV. The 95% confidence level (C.L.) observed and the expected exclusion limits are shown in Table 1 [10]. The combination of the dielectron and dimuon channels is performed under the assumption of lepton universality. The combined limit on the cross-section times branching fraction (σBr) expected from theory is around 0.7 fb and can be read from Fig. 4 of [10]. Since there are no events with dilepton invariant mass above 2 TeV and the DY background is very small, the observed and expected limits are nearly the same.

The ATLAS Collaboration has used the Bayesian approach [20] with a flat, positive prior on the signal cross section to determine an upper limit on the number

Table 1. The observed and expected 95% C.L. lower limits on the mass of the Z^* boson for the $\mu^+\mu^-$ and e^+e^- channels separately and for their combination from [10]

	$Z^* \rightarrow \mu^+\mu^-$	$Z^* \rightarrow e^+e^-$	$Z^* \rightarrow \ell^+\ell^-$
Observed limit, TeV	1.97	2.10	2.20
Expected limit, TeV	1.99	2.13	2.22

of signal events. We will use more simple «number counting» approach for the exclusion limit and the discovery potential evaluations with many other approximations. In particular, we do not use simulation and reconstruction procedure, ignore pileup and experimental systematic uncertainties. Some other approximations we will discuss below in the text. Nevertheless, we will show that our limit estimations are in rather good agreement with the official ATLAS results.

Since any deviation from the Standard Model dilepton distributions is not yet detected, the exclusion limits can only be evaluated. To obtain these limits, we use code `ec1syst.f` [21] which allows one an approximate computation of the confidence level for combined searches with small statistics. The $[M - k\Gamma, M + k\Gamma]$ on-peak region with $k = 3$ has been used for event counting in the electron channel. In the muon channel the same window was used for masses below 2 TeV. For larger masses, the width of the peak is dominated by the resolution of the ATLAS muon spectrometer [10] (the relative resolution is approximately proportional to the resonance mass). Therefore, above 2 TeV the relative window size for the muon channel is scaled accordingly: $k = 3(M/2 \text{ TeV})$. We take into account only the leading Z/γ DY background and neglect many other subdominant backgrounds (like QCD, $t\bar{t}$, diboson and W +jets, etc.).

The number of the expected events, recorded in the detector and passed selection criteria, depends on many factors, which can be expressed through the overall event acceptance \times efficiency ($\mathcal{A}\epsilon$). For the ATLAS detector during 2011 data taking period, the overall event $\mathcal{A}\epsilon$ for a Z' boson with mass 2 TeV decaying into the dielectron final state is about 66%, while for the muon channel this factor is only 43% [10]. To be specific in our estimations, for the ATLAS detector we accept overall event $\mathcal{A}\epsilon = 70\%$ for the electron channel and $\mathcal{A}\epsilon = 40\%$ for the muon channel, both for the signal and for background. We will also assume that these numbers do not depend on the resonance mass.

In order to follow as close as possible to the ATLAS analysis in this section, we use the same parton distribution functions (PDF) set, CTEQ6L1 [22], used by ATLAS for signal generation. Since only the central value is available for the CTEQ6L1 PDF set, the closest set with many PDFs, CTEQ61 [23], is used to estimate systematic PDF uncertainties.

The variation of PDFs has some effect on dependence of production cross section on dilepton mass. Each PDF has a set of independent parameters associated with it. These parameters are known as the eigenvectors of the PDF set in

a function space, as they can be varied in orthogonal directions to quantify the systematic uncertainties associated with the PDF variations.

The CTEQ61 PDF set has 1 central PDF and 20 orthogonal eigenvector variations with a high and low value for each eigenvector. For each eigenvector, the Z^* cross-section times branching fraction is calculated as a function of pole mass in $[M-3\Gamma, M+3\Gamma]$ on-peak region. As far as the program `ec1syst.f` takes into account only symmetric systematic errors, we use only them. The symmetric uncertainty at each mass point is calculated with the equations defined below [23]:

$$(\Delta\sigma)^2 = \frac{1}{4} \sum_{i=1}^{n=20} (\sigma_i^+ - \sigma_i^-)^2, \quad (18)$$

where n is the number of PDF eigenvectors; σ_i^+ is the cross section for the higher value of the i th PDF eigenvector; σ_i^- is the cross section for the lower value of the i th PDF eigenvector. The results are shown in Table 2.

We assume that the PDF uncertainties dominate all other uncertainties at high dilepton invariant masses. Therefore, we use only them as main systematic uncertainties. Using program `ec1syst.f` [21], we get the following limits on Z^* mass: 2.01 TeV in the muon channel and 2.12 TeV in the electron channel. Their combination excludes at 95% confidence level Z^* masses below 2.25 TeV and $\sigma\text{Br} > 0.7$ fb. The obtained results are very close to the official ATLAS results (given in Table 1). This convinces us to use our approach to investigate the LHC potential in searching for the Z^* boson at higher center-of-mass energies.

Table 2. Z^* signal and the Standard Model DY background cross-sections times branching fraction in $[M-3\Gamma, M+3\Gamma]$ on-peak region and maximal relative uncertainty due to PDF variation (at 90% C.L.) with CTEQ61 set

Z^* mass, GeV	Signal		Background	
	σBr , fb	$\Delta\sigma/\sigma$, %	σBr , ab	$\Delta\sigma/\sigma$, %
250	64866.0	5.1	355660.0	4.4
500	4608.2	7.0	25418.0	5.4
750	779.58	9.5	4535.2	6.4
1000	184.29	11.9	1139.9	7.4
1250	51.121	15.4	341.61	8.4
1500	15.436	19.3	113.85	10.7
1750	4.8631	24.9	40.702	13.6
2000	1.5652	32.1	15.248	17.5
2250	0.50793	41.9	5.8910	22.1
2500	0.16543	54.8	2.3148	27.7
2750	0.053988	72.0	0.91438	34.5
3000	0.017720	93.3	0.35945	42.8
3250	0.0058534	118.4	0.13933	53.1
3500	0.0019359	146.6	0.052909	65.8

It should be noted that accounting of the systematic uncertainties is very important. However, since the background is very small in comparison with the signal, main effect of systematics comes from the signal uncertainties. Neglecting in systematics leads to up to 60 GeV weaker limits on the resonance mass in individual channels and up to 30 GeV in their combination.

4. EXCLUSION LIMITS AT $\sqrt{s} = 8$ TeV

In 2012, the ATLAS experiment recorded 20 fb⁻¹ of good data both in dielectron and dimuon final-state channels at $\sqrt{s} = 8$ TeV. Again good agreement between the data and the SM background expectation was found [24]. However, limits only on the Z' Sequential Standard Model boson, E_6 gauge bosons and a spin-2 Randall–Sundrum graviton have been set so far. There are still no events observed by ATLAS [24] above 2 TeV dilepton invariant mass and the observed and expected limits are nearly the same.

In this paper, we precede the official ATLAS results on the excited boson search and evaluate exclusion limits on Z^* at $\sqrt{s} = 8$ TeV. Our analysis is fulfilled in the same way as in the previous section. The only difference, that we use here for the signal and background generation more recent MSTW2008lo PDF set [25]. The corresponding PDF systematics are presented in Table 3.

Table 3. Z^* signal and the Standard Model DY background cross-sections times branching fraction in $[M - 3\Gamma, M + 3\Gamma]$ on-peak region and relative uncertainty due to PDF variation (at 90% C.L.) with MSTW2008lo90cl set

Z^* mass, GeV	Signal		Background	
	σBr , fb	$\Delta\sigma/\sigma$, %	σBr , ab	$\Delta\sigma/\sigma$, %
250	75011.0	3.1	408120.0	2.5
500	5657.3	4.2	30944.0	3.4
750	1044.4	5.5	6049.3	4.3
1000	272.90	6.9	1684.5	5.3
1250	84.302	8.7	562.48	6.5
1500	28.493	10.3	208.89	7.8
1750	10.090	12.0	83.116	9.4
2000	3.6597	14.2	34.575	11.3
2250	1.3414	16.6	14.809	13.7
2500	0.49204	19.8	6.4583	16.3
2750	0.17993	23.5	2.8387	19.5
3000	0.065599	28.2	1.2481	22.8
3250	0.023814	33.1	0.54635	26.2
3500	0.0086385	37.4	0.23602	29.7
3750	0.0031289	40.6	0.10036	33.3
4000	0.0011286	42.0	0.041827	36.8

Figure 6 shows the 95% C.L. expected exclusion limits on σBr for the electron and muon channels. The combined limit is shown in Fig. 7.

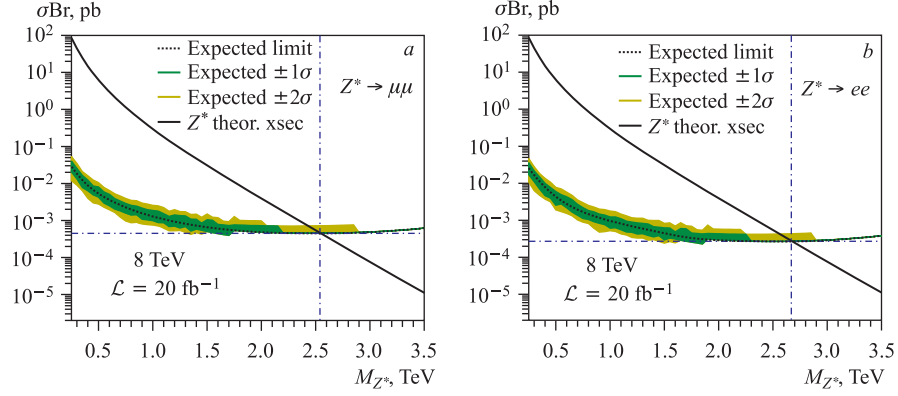


Fig. 6. Exclusion limits from muon (a) and electron (b) channels with 20 fb^{-1} of integrated luminosity at $\sqrt{s} = 8 \text{ TeV}$

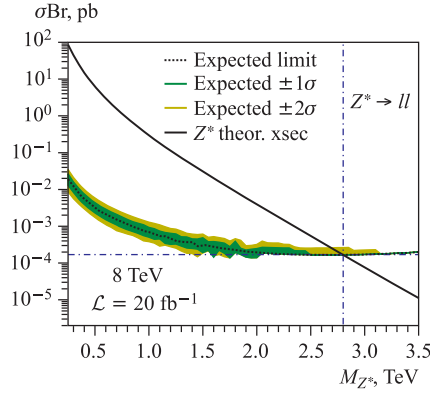


Fig. 7. Combined exclusion limits with 20 fb^{-1} of integrated luminosity at $\sqrt{s} = 8 \text{ TeV}$

Table 4 summarizes constraints on the Z^* boson mass M and production cross section σBr obtained in our approach for $\sqrt{s} = 8 \text{ TeV}$.

Table 4. The expected 95% C.L. limits on the mass and the cross-section times branching fraction of the Z^* boson for the $\mu^+\mu^-$ and e^+e^- channels separately and for their combination at $\sqrt{s} = 8 \text{ TeV}$

Expected limit	$Z^* \rightarrow \mu^+\mu^-$	$Z^* \rightarrow e^+e^-$	$Z^* \rightarrow \ell^+\ell^-$
$M, \text{ TeV}$	2.55	2.67	2.80
$\sigma\text{Br}, \text{ fb}$	0.45	0.27	0.17

5. THE DISCOVERY POTENTIAL AND THE EXCLUSION LIMITS AT $\sqrt{s} = 13$ TeV AND $\sqrt{s} = 14$ TeV

In 2015, the LHC will increase the center-of-mass energy up to the designed value of 14 TeV. In this section, we will estimate the discovery potential and the exclusion limit for the Z^* boson, if no any deviation from the Standard Model expectation will be observed at these energies. For discovery potential estimation we use Eq. (11) with $S_{\text{CL}} = 5$. At the first stage, the center-of-mass energy could be equal to 13 TeV. Therefore, we first consider this possibility using our approach.

The Z^* -production cross sections and PDF systematic uncertainties for 13 TeV are presented in Table 5. Figure 8 shows the luminosity dependences of the relevant discovery potential and exclusion limits for different Z^* masses and all Z^* -decay channels at 13 TeV. It is interesting to note that the higher

Table 5. Z^* signal and the Standard Model DY background cross-sections times branching fraction in the $[M - 3\Gamma, M + 3\Gamma]$ on-peak region and relative uncertainty due to PDF variation (at 90% C.L.) with MSTW2008lo90cl set at $\sqrt{s} = 13$ TeV

Z^* mass, TeV	Signal		Background	
	σBr , ab	$\Delta\sigma/\sigma$, %	σBr , zb	$\Delta\sigma/\sigma$, %
2.0	32645.0	8.5	217260.0	6.4
2.5	8500.8	10.6	63858.0	8.1
3.0	2369.6	12.9	20720.0	10.2
3.5	679.60	15.8	7125.2	12.8
4.0	196.25	19.9	2534.3	16.1
4.5	56.554	25.4	914.46	19.9
5.0	16.214	32.5	330.30	24.0
5.5	4.6351	40.6	117.88	28.3
6.0	1.3211	49.2	41.176	32.6
6.5	0.37523	57.8	13.968	36.9

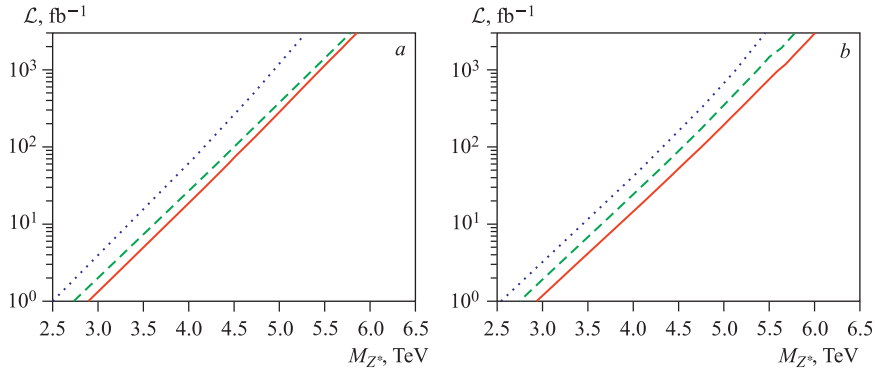


Fig. 8. The Z^* -boson discovery potential (a) and expected 95% C.L. exclusion limits (b) at $\sqrt{s} = 13$ TeV from muon (dotted), electron (dashed) and combined (solid) channels

center-of-mass energy at Run 2 allows one to probe the higher resonance masses than at Run 1 already with 1 fb^{-1} of integrated luminosity.

The designed $\sqrt{s} = 14 \text{ TeV}$ requires new templates and systematics (see Table 6), which only slightly deviates from the previous case of 13 TeV. The final results at 14 TeV for discovery potential and exclusion limits are presented in Fig. 9.

In particular, the LHC Run 2 allows one to discover the Z^* boson with mass up to about 5.3 TeV or to exclude this boson with mass of 5.5 TeV, in case of its signal absence. The High Luminosity LHC with 3000 fb^{-1} of an integrated statistics can extend that reach in the case of a signal-to-mass of about 6.2 TeV for discovery or exclude it up to mass of about 6.4 TeV.

Let us note that effect of systematics is very important at high integrated statistics. So, the constraints on the resonance mass are relaxed up to 150 GeV at 3000 fb^{-1} in the individual channels and up to 100 GeV in the combined channel.

Table 6. Z^* signal and the Standard Model DY background cross-sections times branching fraction in $[M - 3\Gamma, M + 3\Gamma]$ on-peak region and relative uncertainty due to PDF variation (at 90% C.L.) with MSTW2008lo90cl set at $\sqrt{s} = 14 \text{ TeV}$

Z^* mass, TeV	Signal		Background	
	$\sigma\text{Br, ab}$	$\Delta\sigma/\sigma, \%$	$\sigma\text{Br, zb}$	$\Delta\sigma/\sigma, \%$
2.5	11603.	9.8	83291.0	7.5
3.0	3471.3	11.8	28383.0	9.3
3.5	1.0776	14.1	10295.0	11.5
4.0	339.13	17.1	3881.4	14.2
4.5	106.88	20.9	1496.3	17.4
5.0	33.566	25.8	580.80	21.1
5.5	10.502	31.2	225.02	24.9
6.0	3.2794	36.4	86.134	28.9
6.5	1.0229	40.1	32.344	32.9
7.0	0.31737	41.5	11.820	36.9

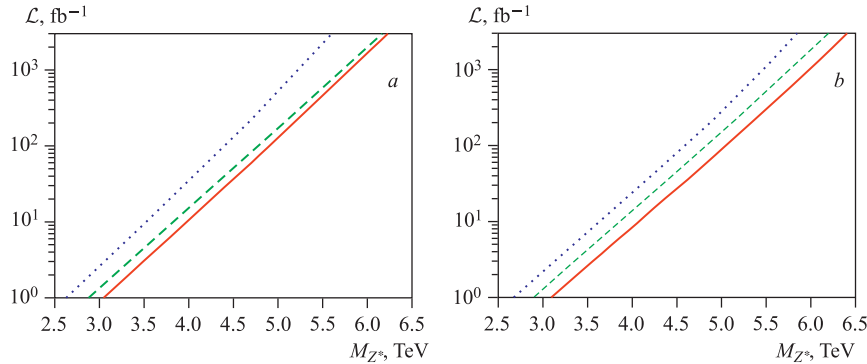


Fig. 9. The Z^* -discovery potential (a) and the expected 95% C.L. exclusion limits (b) at $\sqrt{s} = 14 \text{ TeV}$ from muon (dotted), electron (dashed), and combined (solid) channels

6. THE DISCOVERY POTENTIAL AND THE EXCLUSION LIMITS AT $\sqrt{s} = 33$ TeV

Finally, we will investigate also the discovery potential and the exclusion limits for the excited boson search in the case of the highest center-of-mass energy, $\sqrt{s} = 33$ TeV. The corresponding data for the analysis within our approach are given in Table 7.

The discovery potential and the exclusion limits on the excited boson resonance mass depending on the integrated luminosity are presented in Fig. 10. The plots show that the High Energy LHC can probe two times heavier Z^* -resonance masses at the total integrated statistics which will be available at Run 2.

Table 7. Z^* signal and the Standard Model DY background cross-sections times branching fraction in $[M - 3\Gamma, M + 3\Gamma]$ on-peak region and relative uncertainty due to PDF variation (at 90% C.L.) with MSTW2008lo90cl set at $\sqrt{s} = 33$ TeV

Z^* mass, TeV	Signal		Background	
	$\sigma\text{Br, ab}$	$\Delta\sigma/\sigma, \%$	$\sigma\text{Br, zb}$	$\Delta\sigma/\sigma, \%$
4.5	8741.9	7.7	56120.0	5.7
5.5	2824.5	9.3	19769.0	7.0
6.5	979.46	10.9	7604.7	8.4
7.5	353.68	12.7	3099.7	10.1
8.5	130.17	14.9	1313.1	12.1
9.5	48.328	17.5	570.54	14.6
10.5	17.979	20.9	251.65	17.4
11.5	6.681	24.9	111.70	20.4
12.5	2.4767	29.4	49.630	23.7
13.5	0.91592	33.9	21.899	27.0

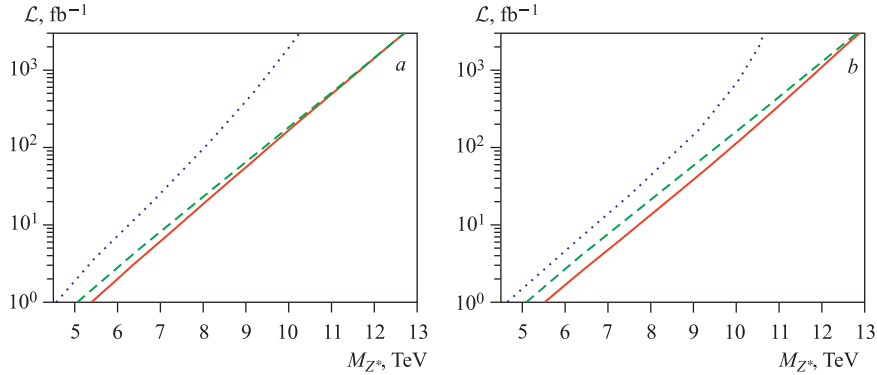


Fig. 10. The Z^* -discovery potential (a) and the expected 95% C.L. exclusion limits (b) at $\sqrt{s} = 33$ TeV from muon (dotted), electron (dashed) and combined (solid) channels

CONCLUSION

Future High Luminosity (HL) and High Energy (HE) program of the LHC is very promising and very exciting. To say nothing about inevitable continuation of the SUSY particle searches, a lot of new particles and new phenomena, in particular, many kinds of exotic heavy resonances, have been proposed for the program.

The neutral Z' bosons of different nature have a long history of their experimental search, and prospects for their investigation with HL-LHC and HE-LHC are well studied due to the most clear signature of their decays into e^+e^- and $\mu^+\mu^-$ dilepton final states.

In fact, these dilepton final states are also very useful for investigation of a new kind of heavy neutral resonances, the excited neutral Z^* bosons which, contrary to the Z' bosons, have only anomalous couplings with the matter and possess different angular distributions for decay products. The Z^* bosons together with W^* bosons are both well theoretically motivated and obviously have to be searched for with future HL-LHC and HE-LHC.

In this paper, we have considered the discovery potential and the exclusion limits on the neutral Z^* excited boson search in pp collisions at the LHC for the different center-of-mass energies and different luminosities.

In particular, we show that the LHC Run 2 can discover the Z^* boson with its mass up to ~ 5.3 TeV, while the HL-LHC can extend this reach up to mass of ~ 6.2 TeV. Furthermore, the HE-LHC can study the Z^* bosons with two times heavier resonance masses at the same integrated luminosity. The field for Z^* boson search remains widely open both at the HL-LHC and the HE-LHC.

REFERENCES

1. Barate R. *et al.* (*ALEPH Collab.*). Search for Evidence of Compositeness at LEP I // Eur. Phys. J. C. 1998. V. 4. P. 571;
Abbiendi G. *et al.* (*OPAL Collab.*). Search for Charged Excited Leptons in e^+e^- Collisions at $\sqrt{s} = 183-209$ GeV // Phys. Lett. B. 2002. V. 544. P. 57;
Achard P. *et al.* (*L3 Collab.*). Search for Excited Leptons at LEP // Phys. Lett. B. 2003. V. 568. P. 23;
Abdallah J. *et al.* (*DELPHI Collab.*). Search for Excited Leptons in e^+e^- Collisions at $\sqrt{s} = 189-209$ GeV // Eur. Phys. J. C. 2006. V. 46. P. 277.
2. Adloff C. *et al.* (*H1 Collab.*). Search for Excited Electrons at HERA // Phys. Lett. B. 2002. V. 548. P. 35;
Chekanov S. *et al.* (*ZEUS Collab.*). Searches for Excited Fermions in ep Collisions at HERA // Phys. Lett. B. 2002. V. 549. P. 32.
3. Acosta D. *et al.* (*CDF Collab.*). Search for Excited and Exotic Electrons in the $e\gamma$ Decay Channel in $p\bar{p}$ Collisions at $\sqrt{s} = 1.96$ TeV // Phys. Rev. Lett. 2005. V. 94. P. 101802;

- Abazov V. M. et al. (D0 Collab.). Search for Excited Electrons in $p\bar{p}$ Collisions at $\sqrt{s} = 1.96$ TeV // Phys. Rev. D. 2008. V. 77. P. 091102.*
4. *ATLAS Collab. Search for Excited Electrons and Muons in $\sqrt{s} = 8$ TeV Proton-Proton Collisions with the ATLAS Detector // New J. Phys. 2013. V. 15. P. 093011; arXiv:1308.1364 [hep-ex];
CMS Collab. Search for Excited Leptons in pp Collisions at $\sqrt{s} = 7$ TeV // Phys. Lett. B. 2013. V. 720. P. 309; arXiv:1210.2422 [hep-ex].*
 5. *ATLAS Collab. Search for New Physics in the Dijet Mass Distribution Using 1 fb^{-1} of pp Collision Data at $\sqrt{s} = 7$ TeV Collected by the ATLAS Detector // Phys. Lett. B. 2012. V. 708. P. 37; arXiv:1108.6311 [hep-ex];
CMS Collab. Search for Narrow Resonances Using the Dijet Mass Spectrum in pp Collisions at $\sqrt{s} = 8$ TeV // Phys. Rev. D. 2013. V. 87. P. 114015; arXiv:1302.4794 [hep-ex].*
 6. *Chizhov M. V., Bednyakov V. A., Budagov J. A. Proposal for Chiral Bosons Search at LHC via Their Unique New Signature // Phys. At. Nucl. 2008. V. 71. P. 2096–2100; arXiv:0801.4235 [hep-ph].*
 7. *Chizhov M. V. New Tensor Particles from $\pi^- \rightarrow e^- \bar{\nu} \gamma$ and $K^+ \rightarrow \pi^0 e^+ \nu$ Decays // Mod. Phys. Lett. A. 1993. V. 8. P. 2753–2762; hep-ph/0401217; Production of New Chiral Bosons at Tevatron and LHC. hep-ph/0609141.*
 8. *Chizhov M. V., Dvali Gia. Origin and Phenomenology of Weak-Doublet Spin-1 Bosons // Phys. Lett. B. 2011. V. 703. P. 593–598; arXiv:0908.0924 [hep-ph].*
 9. *Chizhov M. V. A Reference Model for Anomalously Interacting Bosons // Phys. Part. Nucl. Lett. 2011. V. 8. P. 512–516; arXiv:1005.4287 [hep-ph].*
 10. *ATLAS Collab. Search for High-Mass Resonances Decaying to Dilepton Final States in pp Collisions at $\sqrt{s} = 7$ TeV with the ATLAS Detector // JHEP. 2012. V. 11. P. 138; arXiv:1209.2535 [hep-ex].*
 11. *ATLAS Collab. ATLAS Search for a Heavy Gauge Boson Decaying to a Charged Lepton and a Neutrino in pp Collisions at $\sqrt{s} = 7$ TeV // Eur. Phys. J. C. 2012. V. 72. P. 2241; arXiv:1209.4446 [hep-ex].*
 12. *Chizhov M. V., Bednyakov V. A., Budagov J. A. On Resonance Search in Dilepton Events at the LHC // Phys. Part. Nucl. Lett. 2013. V. 10. P. 144–146; arXiv:1109.6876 [hep-ph].*
 13. *Chizhov M. V., Bednyakov V. A., Budagov J. A. On Resonance Search in Dijet Events at the LHC // Phys. At. Nucl. 2012. V. 75. P. 90; arXiv:1106.4161 [hep-ph].*
 14. *Belyaev A., Christensen N. D., Pukhov A. CalcHEP 3.4 for Collider Physics within and beyond the Standard Model // Comp. Phys. Commun. 2013. V. 184. P. 1729–1769; arXiv:1207.6082 [hep-ph].*
 15. *Bondarenko M. et al. High Energy Physics Model Database: Towards Decoding of the Underlying Theory (within «Les Houches 2011: Physics at TeV Colliders New Physics Working Group Report»). arXiv:1203.1488 [hep-ph]; <https://hepmbd.soton.ac.uk>.*

16. *Hays C. P., Kotwal A. V., Stelzer-Chilton O.* New Techniques in the Search for Z' Bosons and Other Neutral Resonances // *Mod. Phys. Lett. A.* 2009. V. 24. P. 2387–2403; arXiv:0910.1770 [hep-ex].
17. *Bayatian G. L. et al. (CMS Collab.).* CMS Technical Design Report. V. II: Physics Performance // *J. Phys. G.* 2007. V. 34. P. 995.
18. *Chizhov M. V., Bednyakov V. A., Budagov J. A.* Anomalously Interacting Extra Neutral Bosons // *Nuovo Cim. C.* 2010. V. 33. P. 343–350; arXiv:1005.2728 [hep-ph].
19. *ATLAS Collab.* Search for High Mass Dilepton Resonances in pp Collisions at $\sqrt{s} = 7$ TeV with the ATLAS Experiment // *Phys. Lett. B.* 2011. V. 700. P. 163–180; arXiv:1103.6218 [hep-ex].
20. *Caldwell A., Kollar D., Kroninger K.* BAT: The Bayesian Analysis Toolkit // *Comp. Phys. Commun.* 2009. V. 180. P. 2197; arXiv:0808.2552 [physics.data-an].
21. *Junk T.* Confidence Level Computation for Combining Searches with Small Statistics // *Nucl. Instr. Meth. A.* 1999. V. 434. P. 435–443; hep-ex/9902006.
22. *Pumplin J. et al.* New Generation of Parton Distributions with Uncertainties from Global QCD Analysis // *JHEP.* 2002. V. 07. P. 012; hep-ph/0201195.
23. *Stump D. et al.* Inclusive Jet Production, Parton Distributions, and the Search for New Physics // *JHEP.* 2003. V. 10. P. 046; hep-ph/0303013.
24. *ATLAS Collab.* Search for High-Mass Dilepton Resonances in 20 fb^{-1} of pp Collisions at $\sqrt{s} = 8$ TeV with the ATLAS Experiment. ATLAS-CONF-2013-017.
25. *Martin A. D. et al.* Parton Distributions for the LHC // *Eur. Phys. J. C.* 2009. V. 63. P. 189–285; arXiv:0901.0002 [hep-ph].